frequency of microexplosions for working mode of FIHIF reactor. It means that the equation can be written as:

$$v\rho C_v \frac{\partial T}{\partial y} \approx \frac{v\rho Q}{y} = \frac{\rho Q}{\tau},$$

where v—velocity of coolant flow, Q—heat quantity, emitted during the microexplosion, τ—period between microexplosions. The shceme of how this artificial convection works is presented on the Fig. 4.

Results. All computational tests were made on the programm compiled from fortran-77 code written according to the given model and conditions.

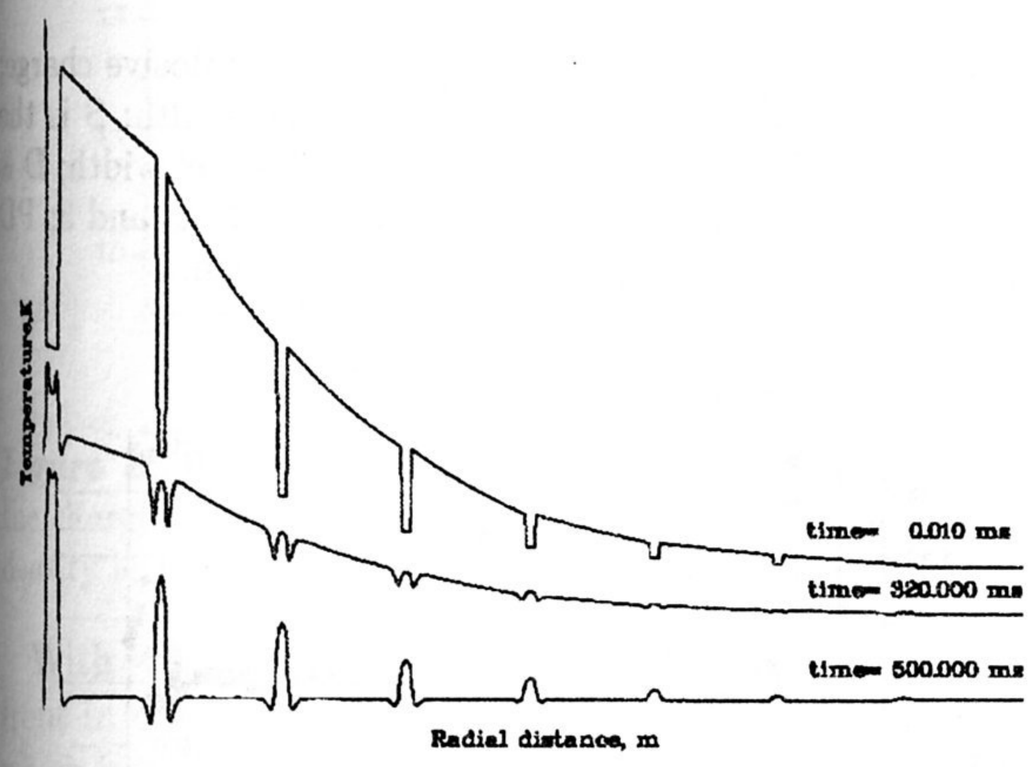

Figure 5. Results of calculations with the use of convection.

Fig. 5 shows the result of using artifical convective heat emission in the calculations. As it was assumed the heat in coolant is carried away within 500 msec. Dips of temperature can be seen on the figure near walls. It is explained by the rough model of convection, thus making the initial fast change of temperature near walls to be saved up to the end of the given period of time, when convection works.

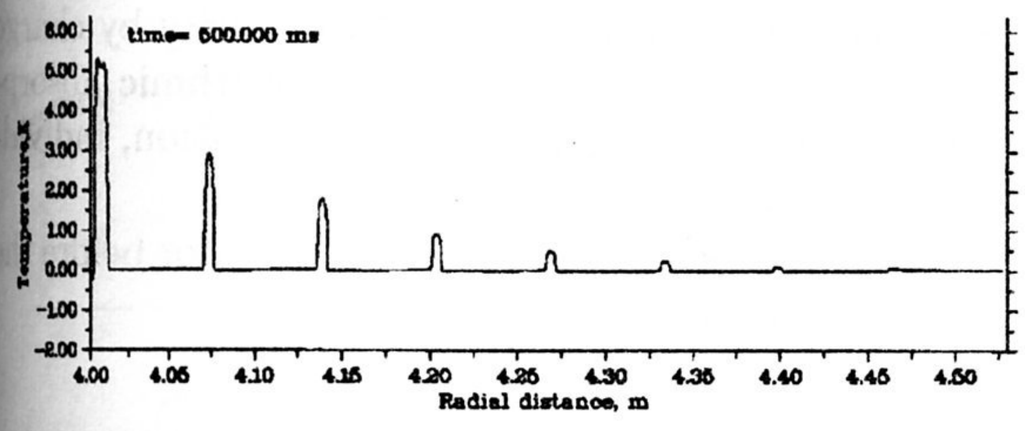

Figure 6. Results of calculations with the correction to the convection.

To get rid of this dips we use mathematical method consisting of bringing in the correction coefficient α. This coefficient is calculated according to the given expression:

$$\alpha = \frac{T_j}{T_{middle}}.$$

To get the desired result we multiply this coefficient by convective part. The result can be seen on the figure 6.

After all corrections were made we calculated the change of temperature in working mode of reactor, when the microexplosions are repeated every 500 msec heating the blanket. The results are shown on the figure 7.

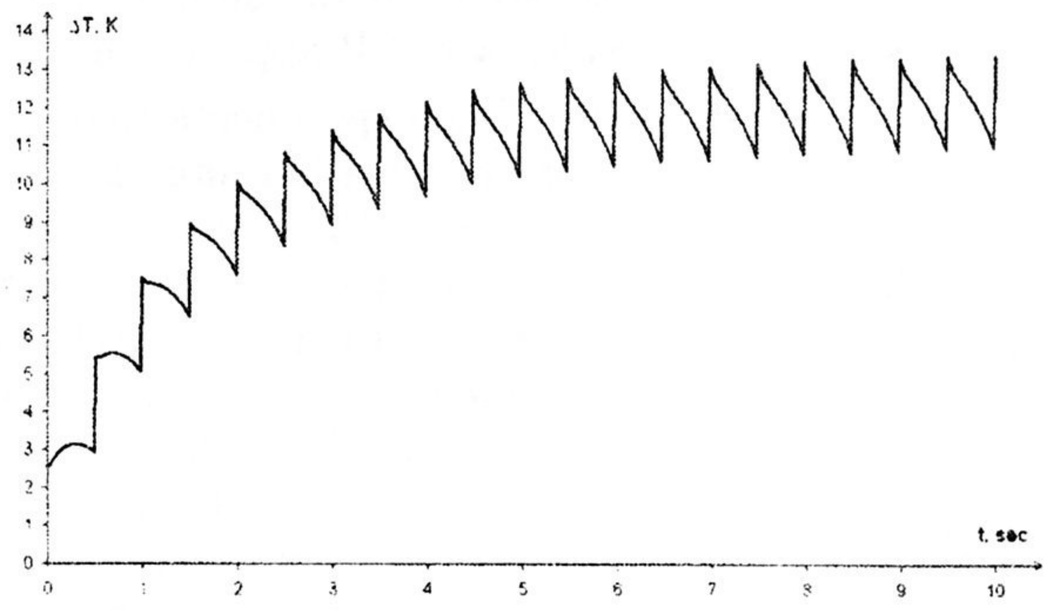

Figure 7. Temperature in the middle of first wall depending on time.

Conclusions. Numerical calculations of unsteady temperature fields in the blanket of FIHIF reactor that were made show that for suggested construction of blanket with given frequency of microexplosions, which is a demand for such type of energy plants, the reactor is able to work in frequency mode in the constant range of temperatures without overheating.

1. Medin S.A. et al. Power plant conceptual design for fast ignition heavy ion fusion // Nuclear Instruments and Methods in Physics Research A 544, 2005, P.300-309.
2. GROUP-6, MCNP-A General Monte Carlo Code for Neutron and Photon Transport, LA-7396-m revised, Los Alamos National Laboratory, April 1981

DIAGNOSTICS OF DENSITY DISTRIBUTION ON THE DETONATION WAVE FRONT USING SYNCHROTRON RADIATION

Ten K.A.*[*1], Zhogin I.L.[2], Lukyanchikov L.A.[1], Pruuel E.R.[1], Titov V.M.[1], Tolochko B.P.[2]

[1]LIH SB RAS, [2]ISSCM SB RAS, Novosibirsk,

**ten@hydro.nsc.ru*

Abstract. A new method of remote measurement of density distribution on the detonation wave front with registration of passed synchrotron radiation (SR) intensity has been realized. SR was registered by a gaseous detector DIMEX with a resolution of 100 μm. Methods to restore density from measured intensity of passed radiation are presented as well as density distributions obtained for pressed hexogen.

Introduction. The classical detonation theory implies a shock jump followed by a zone of chemical reaction, where pressure decreases and the substance extends up to the Chapman-Jouguet parameters. Information on processes in the reaction zone is very limited, first of all, because of its small size (less than 1 mm), high velocity of defining processes ($\sim 0.1\,\mu$s), and ultimate aggressivity of the medium. At the same time, some of processes evolving in this zone are not easy to realize under other conditions. Those are chemical transformations at high pressures and temperatures, phase transitions, etc. The available methods of measurement of substance parameters in the chemical reaction zone either perturb the process to measure (pressure transducers) or use an intermediate substance (foil or bromoform). It is the velocity of explosive charge end movement that can be measured most accurately. A promising method of non-perturbing remote measurement of substance parameters including density is x-ray diagnostics with SR application [1, 2].

Experimental setup. The experiments were carried out at the station for investigation into explosive processes on the basis of the VEPP-3 accelerator at Budker Institute of Nuclear Physics SB RAS. Pressed hexogen, trotyl, and mixtures of them were under investigation. Before experiments, all the high explosives were recrystallized using acetone. The explosive charges were 15 mm in diameter and 8 to 10 calibres in length. The explosive charges were initiated with an explosive lens as light as 5 g. The explosive charge (E) was placed horizontally (Fig. 1) along the shaped SR beam with a height of 0.4 mm and width H = 18 mm. The axis of the explosive charge to investigate lay in the SR beam plane. The detonation front (D) passed sequentially positions 1, 2 and 3, staying in the SR beam zone for 3 to 4 μs. This time allowed taking 3 to 5 shots (with an exposure of 1 ns) of distribution of passed radiation along the charge axis. Time between frames was defined by the period of beam rotation in the accelerator and was 250 to 500 ns. The detector DIMEX (S), which was also placed along the charge axis 770 mm from object E, was registering the radiation. The registration channels were 1 mm in height and 0.1 mm along the charge axis. The total number of channels was 256 (25.6 mm). The detector was triggered when a contact sensor mounted on the explosive lens got closed.

Experimental results. Fig. 2 presents three frames of relative intensity variation (the measured intensity divided by the initial one) along the charge axis at detonation of pressed trotyl. Detonation spreads towards first detector channels. The time between the first (B) and third (D) frames is 1 s. The detonation velocity found from the front movement was D = 8.3 km/s. The charge diameter was 15 mm; its length was 80 mm. The region to study was 10 mm from the charge end.

During detonation of the explosive and subsequent scatter of explosion products, substance density along the SR beam varies significantly and therefore so does the absorption spectrum. For RDX and other high explosives, absorption by the detector DIMEX was calibrated depending on the product of density by charge thickness ($Y = \rho d$, g/cm^2). The logarithmic absorption was subjected to parabolic interpolation, individual for each of the detector channels.

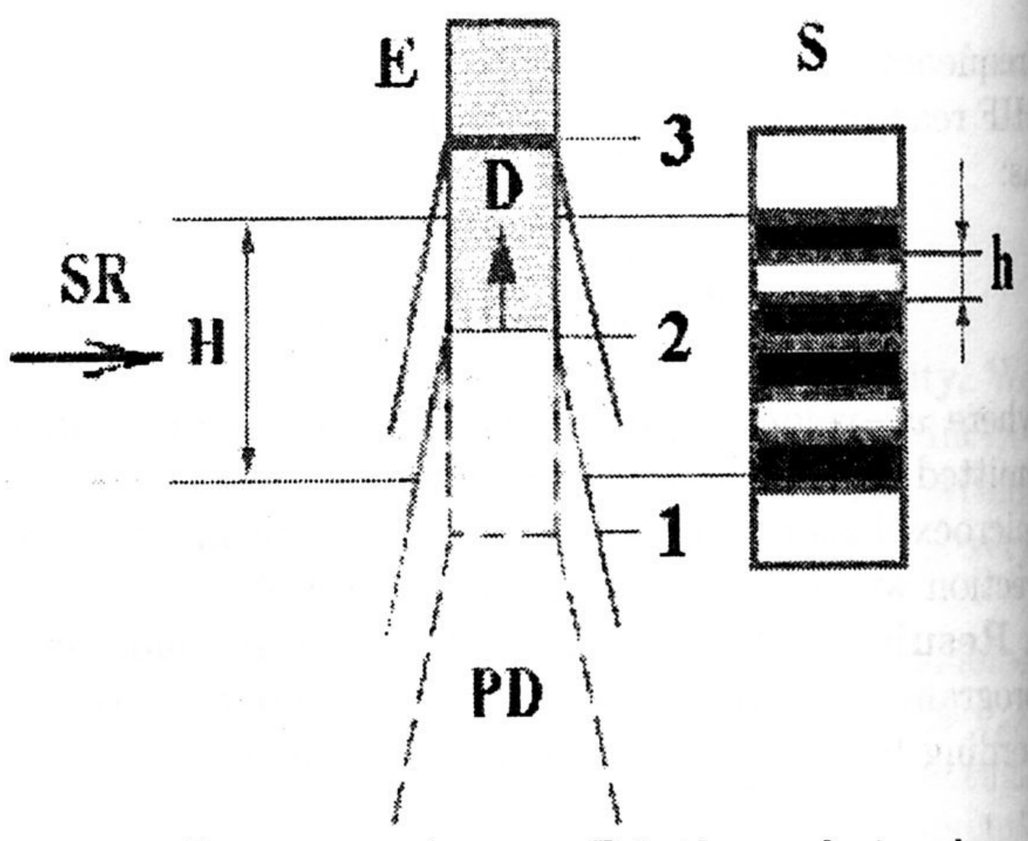

Figure 1. Experimental setup. E is the explosive charge; SR is the SR beam plane; H is the beam width; S is the detector DIMEX; h is the registration channel width; D is the detonation front position at moments 1, 2, and 3; PD denotes the scattering products of detonation.

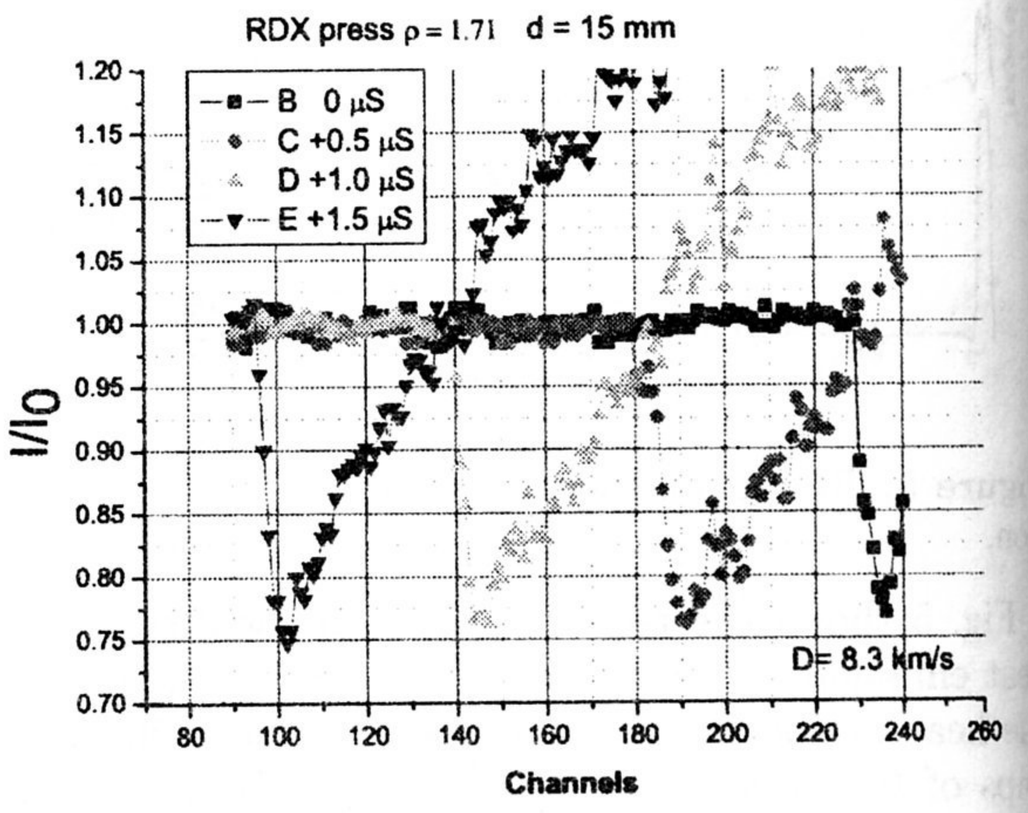

Figure 2. Relative intensity variation along the charge axis at detonation of pressed RDX. Detector channels 0.1 mm wide are plotted along the X axis.

Intensity that is registered by the detector before the experiment can be written as

$$J_{\text{before}} = J_{\text{air}} \exp(-\alpha_1 m_0 + \alpha_2 m_0^2),$$

where J_{air} is the initial SR flux, m_0 the mass of the substance along the SR beam ($m_0 = Y = \rho_0 d_0$, where ρ_0 is the initial density and d_0 is the charge diameter), α_1, α_2 are the interpolated coefficients of absorption. Intensity that is registered by the detector during the experiment can be written as

$$J_{\text{exp}} = J_{\text{air}} \exp(-\alpha_1 m_x + \alpha_2 m_x^2),$$

where m_x is the mass of the substance along the beam.

The logarithm of the J_{exp} to J_{before} ratio equals:

$$\ln \frac{J_{\text{exp}}}{J_{\text{before}}} = g = -\alpha_1 (m_x - m_0) + \alpha_2 (m_x - m_0)^2,$$

whence one can obtain the relative increase in mass on the front:

$$\frac{m_x}{m_0} = \frac{\alpha_1^2}{4\alpha_2^2 m_0^2} - \frac{1}{\alpha_2 m_0}\left(\alpha_1 - \frac{g}{m_0}\right) + 1.$$

The resulting profile of mass variation is presented in Fig. 3.

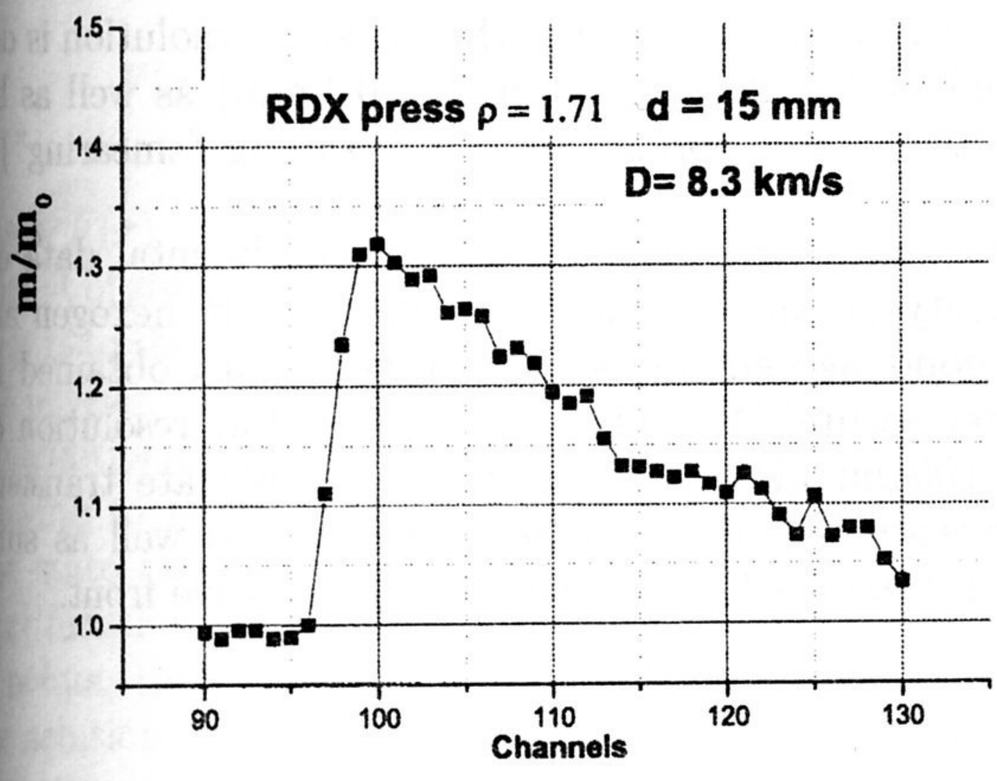

Figure 3. Variation in relative mass on the front along the charge axis at detonation of pressed RDX. The initial density is 1.71 g/cm^3.

With any method of initiation, the detonation wave front in cylindrical charges is curved, the influence of which has to be taken into account. Fig. 4a presents a photo scanning of detonation arrival at the charge end, which was used to find out the convexity X, whence the radius of detonation front curvature was determined. At X = 0.8 mm, the radius of curvature was R = 38 mm.

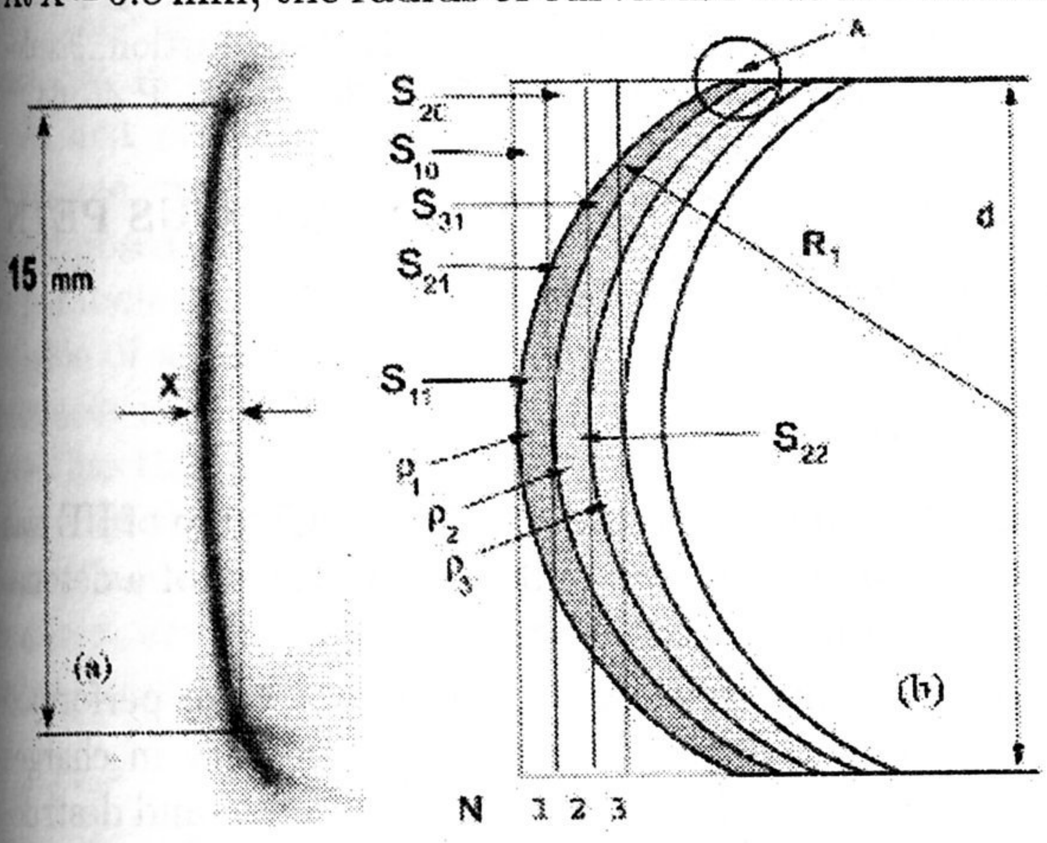

Figure 4. (a) Photo scanning of detonation arrival at the end of the pressed RXD charge of 15 mm in diameter. The convexity X = 0.8 mm; (b) Scheme of computation of density ρ_i on the detonation wave front.

Reconstruction of density distribution on the detonation wave front. Density distribution was computed assuming that the detonation wave front was spherical and density depended on the radius R. The scheme of measurement of mass in first detector channels (from the detonation front) is shown in Fig. 4b. Since the registration zone thickness is defined by the SR beam width and is the same for all channels, mass along the SR beam is determined by the area of strips 1, 2, 3, etc. The S_{11} zone, where density equals ρ_1, is a small part of the volume where the mass m_1 was measured. It is $(S_{11} + S_{10})$h, where h is the thickness of the layer to measure. If densities at distances of h, 2h, and 3h from the detonation front (h is the detector channel width) are designated as ρ_1, ρ_2, and ρ_3, the scheme of density re-computation will be as follows:

$$m_1 = S_{10}\rho_0 + S_{11}\rho_1 \quad \text{– mass in the first channel;}$$

$$m_2 = S_{20}\rho_0 + S_{21}\rho_1 + S_{22}\rho_2 \quad \text{– in the second channel;}$$

$$m_3 = S_{30}\rho_0 + S_{31}\rho_1 + S_{32}\rho_2 + S_{33}\rho_3 \quad \text{– in the third.}$$

Solution of this system of equations allows finding out ρ_1, ρ_2, ρ_3, i.e. determination of density distribution on the detonation wave front. Fig. 5 presents the obtained density distribution on the detonation wave front in pressed RDX.

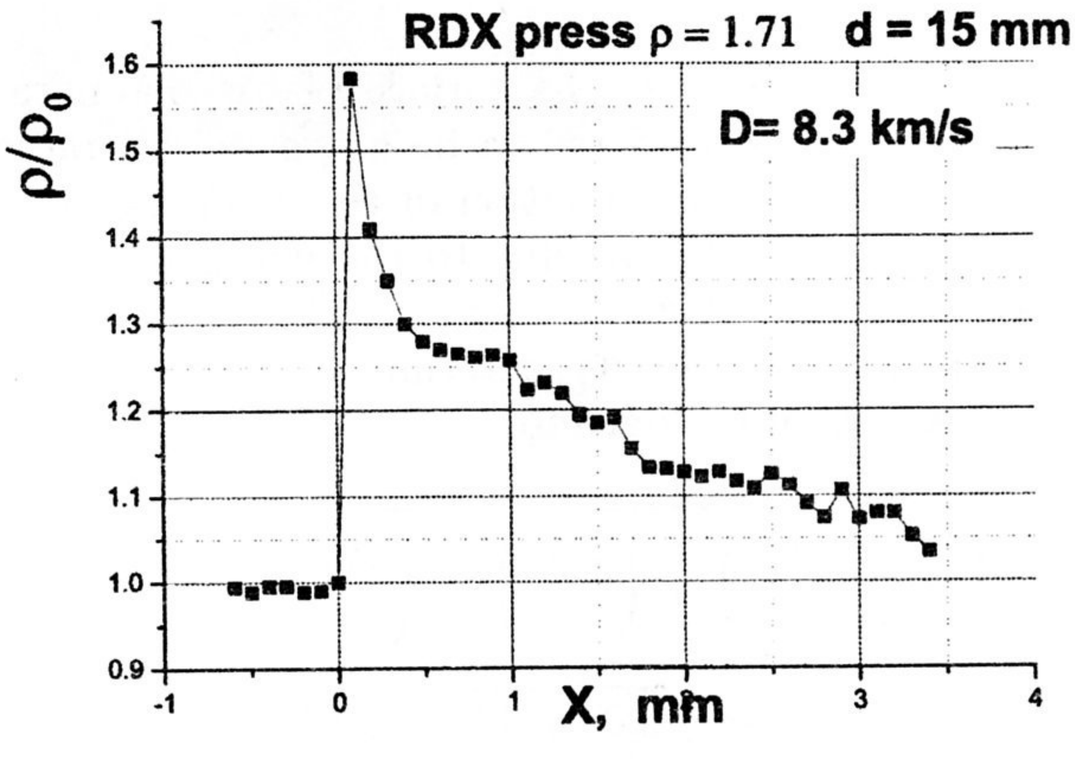

Figure 5. Density distribution on the detonation wave front in pressed RDX.

The detonation front characteristics obtained for RDX and TNT are presented in Table 1, where ρ_N is the maximum density of the von Neumann spike, τ and Δ are the spike duration and width, ρ_{CJ} is the Chapman-Jouguet density, and γ is the polytropic exponent of the products in the Chapman-Jouguet plane. Column Δ_1 presents generalized data on the chemical transformation zone sizes that were obtained by different methods, which are summarized in enough detail in [4]. Parameter $K = \rho_N/\rho_{CJ}$ shows the ratio of the density of the von Neumann spike to that in the Chapman-Jouguet plane.

Comparison of Δ and Δ_1 shows that the reaction zone parameters obtained with SR application verify similar data found with other methods. According to data in [4], $K = 1.3 \pm 0.1$ is enough for big-diameter and big-length charges of most solid dense explosives. We obtained a ratio of values of the Neumann spike and Chapman-Jouguet state ~1.25, which reflects a rather small diameter of charges used in the investigation because, according to [4] and data of other investigators, the charge size influences significantly the effective pressure value in the Chapman-Jouguet plane.

Estimate of the methods accuracy. The accuracy of density determination is defined by the detector reading error ΔJ, mass measurement error during calibration ΔF, error ΔY due to detector reading "smearing", and error Δd caused by uncertainty in the actual

Table 1. Parameters on the detonation wave front in pressed RDX and TNT.

HE	ρ_N, g/cm^3	ρ_{CJ}, g/cm^3	τ, μs	Δ, mm	Δ_1, mm	$\frac{\rho_N}{\rho_{CJ}}$
TNT	2.59	2.09	0.1±0.014	0.7±0.1	0.63–0.97	1.24
RDX	2.7	2.15	0.48±0.012	0.4±0.1	0.36–0.6	1.25

size of the compression region because of detonation front curvature.

The detector reading error ΔJ can be taken $\frac{\Delta J}{J} \approx 2\%$ when averaged over three experiments [3].

It is necessary to add the detector reading correction error ($\approx 1\%$) and the error of mass reconstruction along the SR beam ($\approx 0.8\%$) to this value:

$$\frac{\Delta Y}{Y} \approx 1\%, \ \frac{\Delta F}{F} \approx 0.8\%.$$

In our experiments, the surface of the detonation wave front was considered to be a sphere of a radius R.. The error of determination of the compression region sizes (the value d) due to the detonation front sphericity is $\frac{\Delta d}{d} \approx 3\%$.

Therefore, the density determination error in the first channels of the detector

$$\frac{\Delta\rho}{\rho} = \sqrt{\left(\frac{\Delta J}{J}\right)^2 + \left(\frac{\Delta Y}{Y}\right)^2 + \left(\frac{\Delta Y}{Y}\right)^2 + \left(\frac{\Delta d}{d}\right)^2}$$

$$\approx \sqrt{2.0^2 + 3.0^2 + 0.8^2 + 1^2} = 3.8\,\%$$

This estimation is true up to a channel where side scattering of products is registered. At this instant, the spherical front reaches the side surface of the charge (area A in Fig. 4). Later on, the error caused by the geometry of detonation products scatter and uncertainty in the parameters on the side surface of the explosive charge (in area A) is added.

The above estimates demonstrate a good accuracy of density measurement, while spatial resolution is defined by the detector step (h = 0.1 mm) as well as by electric charge spread inside it (reading "smearing").

Conclusion. The obtained experimental data on density on the detonation wave front in hexogen are in good agreement with literature data obtained in other setups [4]. The observed spatial resolution of $\sim 100\,\mu$m makes it possible to investigate transient processes at initiation of detonation as well as substance parameters on the detonation wave front.

1. Ten K. A., Evdokov O. V., Zhogin I. L. *et al.* // Combustion, Explosion, and Shock Waves. 2007. V. 43, No. 2, P. 204.
2. Ten K. A., Evdokov O. V., Zhogin I. L., Zhulanov V. V., Zubkov P. I., Kulipanov G. N., Luk'yanchikov L. A, Merzhievsky L. A., Pirogov B. Ya., Pruuel E. R., Titov V. M., Tolochko B. P., Sheromov M. A. // NIM A. 2005. V. 543. No. 1. P. 170.
3. Aulchenko V., Zhulanov V., Shekhtman L., Tolochko B., Zhogin I., Evdokov O., Ten K. One-dimensional detector for study of detonation processes with synchrotron radiation beam. // NIM. 2005. V. A543. No. 1. P. 350.
4. Loboiko B. G., Lyubyatinsky S. N. Combustion, Explosion, and Shock Waves. 2000. V. 36. No. 6. P. 45–64.

DENSITY EVOLUTION DURING THE INITIATION OF DETONATION IN POROUS PETN

Pruuel E.R., Kashkarov A.O.*, Lukyanchikov L.A., Merzhievsky L.A.

LIH SB RAS, Novosibirsk,

**kashkarov@hydro.nsc.ru*

The paper deals with the method and results of diagnostics high-velocity nonstationary processes using high-speed X-ray tomography. Investigation of transition from combustion to detonation was performed for porous charges of high explosives (PETN).

As a source of X-ray was used synchrotron radiation. The beam of SR through special windows in the explosive chamber penetrates through an investigated charge and the attenuated radiation gets on the linear detector. Energy of photons much above energy of chemical bonds in substance, therefore influences not chemical structure but only atomic structure of investigated substance. From the linear detector (256 channels with an interval 0.1 mm between them) are taken the data about intensity of the attenuated radiation with an interval in 500 nanosecond (32 shots) at time of an exposition 1 nanosecond. The basic scheme of the detector and research facility is in detail stated in work [1].

The nonstationary flow arising at initiation charge of PETN bulk density in a fragile thin cover was investigated. The size of particles 200–300 micron, charge length 20–30 mm, diameter 16 mm. Charge of HE was initiated by a high-speed flow of products of a detonation of additional HE charge.

Experiments in similar statements were performed earlier repeatedly. Distribution of density in charges and in the field of scattering, deformation and destruction of inert mediums was investigated. Essential difference of experiments in this work is research of detonation in porous HE charge. In this case considerable curvature of front, and a flow essentially nonstationary is observed.

Experiments were made at two various arrangements of HE charge relatively a SR beam: longitudinal and cross-section. The first statement of experiments allows to see the process as a whole from a stage of initiation to development of a stationary detonation in a charge that gives the chance to define dynamics of position and speed of front. The front form and flow structure behind front remain are unknown. The data of cross-section statement is used for tomographic flow visualisation. Sharing of results from both statements allows to reconstruct structure of density distribution

Institutions of the Russian Academy of Sciences
Joint Institute for High Temperatures RAS
Institute of Problems of Chemical Physics RAS
Kabardino-Balkarian State University

Physics of Extreme States of Matter — 2009

Chernogolovka, 2009